AERODYNAMIC ANALYSIS OF GROOVE BASED VORTEX TRAP CONFIGURATION ON THE RETREATING HELICOPTER BLADE

MOHD FAUZI BIN YAAKUB

A thesis submitted in
fulfillment of the requirement for the award of the
Doctor of Philosophy

Faculty of Mechanical and Manufacturing Engineering
Universiti Tun Hussein Onn Malaysia

OCTOBER 2019

ACKNOWLEDGEMENT

Alhamdulillah and ‘syukur’ to Allah s.w.t for His guidance and blessing upon my family and me. He has given me strength, knowledge and patience to complete this study.

I would like to express my deepest gratitude to my supervisor, Dr. Aslam bin Abdullah, and my co-supervisor, Dr. Nik Ahmad Ridhwan Bin Nik Mohd, for their guidance, advice and continuous encouragement that helped me to perform this study successfully. I also would like to extend my sincere gratitude to my late main supervisor, Allahyarham Prof. Ir. Dr. Hj. Abas bin Ab Wahab (A.M.N), for his guidance and support.

Gratitude and appreciation are also extended to my friends and colleagues in UTHM, including Mohammad Fahmi bin Pairan, Mohd Zarif bin Md Shah and Siti Nur Mariani binti Mohd Yunos. It has been an honor and privilege to have met and worked with all of them. To all my friends in the Department of Aeronautical Engineering UTHM, thank you for the dedication and commitment that you have given to patiently answer all the questions needed for this study. Furthermore, I am forever grateful to all my friends who have helped me directly or indirectly while completing this research.

Special thanks to my lovely wife, Nazarul Wahyuni Binti Mohd Mokshim, for her support, understanding and sacrifices during the period of my study. Furthermore, special thanks to my three beautiful daughters, Dahlia Amani, Chempaka Aisya and Mawar Annur. Their smiles and laughter gave me the spirit and strength to complete this study with passion. I am also grateful to my ‘Abah’ Yaakub bin Mat and ‘Mak’ Zainab binti Said for their prayers and unparalleled support.

Finally, I would like to express my appreciation and gratitude to the Ministry of Education Malaysia and Universiti Tun Hussein Onn Malaysia (UTHM) for the opportunity and the financial support offered under Academic Training Scheme (SLAB).

ABSTRACT

The issue of high angle of attacks at the retreating blade receives attention from countless researchers because it is an important factor in the stability of the helicopter. The retreating blade stall will effect the stability of the helicopter due to the high angle of attacks. Prouty's helicopter data are used in this research to study the influence of the groove in the vortex trapped method on the helicopter stability. The method is implemented to control the flow of separation at the rotor blade on the retreating side of the rotor disc in forward flight conditions. One of the codes used to implement the method is the Blade Element Theory Code using Prouty's dataset. The code aids in the analysis of the aerodynamic characteristics of the helicopter main rotor blade. To validate the code, the angle of attack distribution along the main rotor blade in forward flight condition is compared to published data of Prouty's. Another approach is the use of Computational Fluid Dynamics to investigate the flow characteristics and aerodynamic parameters of the baseline helicopter aerofoil and modified helicopter aerofoil with the groove. The data obtained from both approaches are then combined in the analysis of the aerodynamic performance of both main rotor blades with or without the groove in forward flight condition. The influence of groove as a vortex trap is studied by means of the change in lift produced by the blade. The groove configuration is varied to determine its most suitable location, which is the critical sub-area at the retreating blade side, between 0.6*R* to 1.0*R* from the rotor hub, where *R* is the rotor disc radius. It is also found that the groove's location on the blade influences the choice of size. The best groove configuration is at 0.5*c* from the leading edge, with the size of 0.05*c*. The presence of groove affects the lift coefficient as simulated at 0° to 18° blade angle of attack. It is proven that the groove contributes significant aerodynamic capability in controlling the flow separation at high angle of attack. The important implication of this research is that the groove equipped helicopter blade offers an improvement in aerodynamic stability in which the load difference is 2.2% lower than that in the case of baseline blade. The blade also provides extra safety margin where the maximum angle of attack allowed is extra 6 degrees higher.

ABSTRAK

Sudut serang yang tinggi pada bilah undur mendapat perhatian kebanyakan penyelidik, sebagai faktor penting dalam kestabilan sesebuah helikopter. Fenomena tegun bilah undur akan memberi kesan kepada kestabilan helicopter akibat sudut serang yang tinggi. Dalam kajian ini, data helikopter Prouty digunakan bagi mengkaji kesan alur dalam kaedah perangkap vorteks terhadap kestabilan helikopter. Kaedah ini bertujuan mengawal aliran terpisah pada bilah undur helikopter dalam penerbangan ke depan. Satu pendekatan yang digunakan adalah Kod Teori Unsur Bilah yang menggunakan input daripada Prouty. Kod ini membantu dalam analisa ciri-ciri aerodinamik bilah utama helikopter. Bagi menentusahkan kod ini, keputusan taburan sudut serang bilah utama daripada kod ini dibandingkan dengan data output Prouty. Satu lagi pendekatan adalah penggunaan perkomputeran dinamik bendalir bagi mengkaji ciri-ciri aliran dan parameter-parameter aerodinamik bilah piawai, dan bilah yang dilengkapi alur perangkap vortex. Data yang diperolehi daripada kedua-dua kaedah tersebut digabungkan dalam kajian prestasi aerodinamik kedua-dua bilah utama helikopter, samada dilengkapi dengan alur perangkap vorteks atau sebaliknya, dalam penerbangan ke depan. Kesan alur perangkap vorteks dikaji dengan menentukan selisih daya angkat yang dihasilkan oleh kedua-dua bilah. Variasi konfigurasi perangkap vorteks dikaji untuk menentukan lokasi alur yang sesuai; didapati lokasi kritikal di antara 0.6R hingga 1.0R dari hab rotor, di mana R adalah radius bilah. Turut didapati bahawa lokasi alur mempengaruhi saiznya. Konfigurasi alur yang terbaik adalah pada pada 0.5c dari tepi depan airfoil dengan saiz 0.05c. Didapati alur memberi kesan kepada pekali daya angkat pada sudut serang bilah antara 0° hingga 18°. Turut dibuktikan bahawa alur tersebut menyumbang kepada keupayaan mengawal aliran terpisah pada sudut serang yang tinggi. Implikasi penting kajian adalah peningkatan kestabilan aerodinamik bilah helikopter, di mana selisih beban pada kedua-dua bilah adalah 2.2% lebih rendah daripada selisih beban bilah helikopter piawai. Alur pada bilah juga meningkatkan margin keselamatan, di mana sudut serang maksimum yang dibenarkan tambahan 6 darjah lebih tinggi.

TABLE OF CONTENTS

	DECLARATION OF THESIS STATUS	**ii**
	EXAMINER'S DECLARATION	**iii**
	TITLE	**iv**
	STUDENT'S DECLARATION	**v**
	ACKNOWLEDGEMENT	**vi**
	ABSTRACT	**vii**
	ABSTRAK	**viii**
	TABLE OF CONTENTS	**ix**
	LIST OF TABLES	**xiii**
	LIST OF FIGURES	**xv**
	LIST OF SYMBOLS AND ABBREVIATIONS	**xxii**
	LIST OF APPENDICES	**xxvi**
CHAPTER 1	**INTRODUCTION**	**1**
	1.1 Background study	1
	1.2 Problem statement	6
	1.3 Research aim and objectives	7
	1.4 Research scope	8
	1.5 Thesis structure	8
CHAPTER 2	**LITERATURE REVIEW**	**10**
	2.1 The effect of different number of blades of the helicopter main rotor blade	10
	2.2 Helicopter rotor blade tip shapes	12
	2.3 British Experimental Rotor Program (BERP) blade	17
	2.4 CFD simulation on the helicopter	25
	2.5 Previous works on flow control separation on the helicopter	

blade 26
2.6 Vortex trap method 31
2.7 Chapter summary 43

CHAPTER 3 RESEARCH METHODOLOGY 48
3.1 Research methodology flowchart 48
3.1.1 Development of Blade Element Theory Code 50
3.1.2 A Computational Fluid Dynamic analysis 51
3.1.3 Analysis of the aerodynamic performance of the helicopter main rotor blade 52
3.2 Application of the Blade Element Theory on the helicopter blade 52
3.2.1 The importance and aim of analysis using Blade Element Theory 53
3.2.2 Advancing and retreating blade 54
3.2.3 Velocities on the helicopter blade in the forward flight conditions 57
3.2.4 Blade pitch motion 60
3.2.5 Blade flapping motion 63
3.2.6 Rotor angle relationships used in rotor analyses 65
3.2.7 The blade element local angle of attack 67
3.2.8 Closed-form integration for thrust 70
3.2.9 Developing Blade Element Theory Code 71
3.3 The Computational Fluid Dynamic analysis 74
3.3.1 Governing Equations-Navier-Stokes equations 74
3.3.2 The Shear-Stress Transport (SST) $k-\omega$ turbulence model 77
3.3.3 Modelling the turbulence production 80
3.3.4 Flowchart of the simulation process 84
3.3.5 Pre-Processor – Geometry, mesh and boundary conditions 85
3.3.6 Flow solver 94
3.3.7 Post-processor 97
3.4 Chapter summary 98

CHAPTER 4 RESULTS AND DISCUSSIONS **99**

4.1 Aerodynamic analysis of rotor in the forward flight using Blade Element Theory code 100

4.1.1 Case a: Effect of increasing forward speed of the helicopter 105

4.1.2 Case b: The effect of increasing the forward speed and the collective pitch angle, θ_o 107

4.1.3 Case c: Effect of changing the twist angle of the blade, θ_{tw} 111

4.1.4 Location to install the groove on the helicopter blade 115

4.2 Turbulence model analysis 118

4.3 Grid-independent analysis 121

4.3.1 Dimensionless wall distance 121

4.3.2 Boundary layer thickness, δ, and size of the element 124

4.4 Analysis of the groove 127

4.4.1 Analysis of the location of the groove 130

4.4.2 Analysis of radius of the groove 132

4.4.3 The best configuration of location-radius of the groove 135

4.4.4 Flow separation of baseline aerofoil and aerofoil with groove 137

4.4.5 The flow inside the groove and pressure distribution 139

4.5 Aerodynamic performance of the helicopter main rotor blade 142

4.5.1 Relationship between the angle of attack of helicopter and lift coefficient of the vortex traps. 142

4.5.2 Advantage of the groove - Safety margin of the helicopter 145

4.5.3 Advantage of the groove for twist angle of the helicopter blade 146

4.5.4 Advantages of the groove for the angle of collective pitch control 147

4.6 Chapter summary 148

CHAPTER 5 CONCLUSIONS AND RECOMMENDATIONS **150**

5.1 Conclusions 150

5.1.1 Developing a Blade Element Theory Code 151

5.1.2 Investigation of the area on the main rotor blade in order to install the groove when the helicopter is in forward flight motion 151

5.1.3 Determination of the best location and the size of the radius of the groove at the helicopter main rotor blade 153

5.1.4 Investigation of the aerodynamic performance between baseline helicopter main rotor blade and modified helicopter main rotor blade with the groove 155

5.2 Significant contribution of the research 156

5.3 Recommendations for future work 157

REFERENCES **159**

APPENDIX **168**

LIST OF TABLES

2-1	Advantages of a low and high number of blades	11
2-2	Comparison of the flow separation between fixed-wing and rotary wing of BERP blade at angle of attack 20 degrees	22
2-3	Summary of previous works of vortex trap method and the research gap	44
3-1	Blade parameter and Prouty's data used for analysis.	72
3-2	Solver and viscous model setting	96
3-3	Boundary conditions and references value	96
3-4	Solution methods	97
4-1	Lift per running meter at advancing and retreating side.	103
4-2	Location to install the groove	116
4-3	One and Two-Equation turbulence models	118
4-4	y^+ variations with respect to the mesh of first cell distance from wall for NACA 0012 aerofoil M = 0.35, Re = 3x10^6	121
4-5	Difference in the lift coefficient between experimental and numerical results obtained for three meshes used in evaluating mesh sensitivity for NACA 0012 aerofoil M = 0.35, Re = 3x10^6	123
4-6	The size of elements and inflation mesh α = 10deg, M =0.4	125
4-7	The dimension of the location and size of the groove at the blade tip, r/R =1.0	127
4-8	Analysis of location and radius of the groove on the main rotor blade	128
4-9	The lift force per running length, $\Delta L/\Delta r$, at the advancing blade for baseline blade and blade with the groove	143
4-10	The lift force per running length, ΔL/Δr, at the retreating	

	blade for baseline blade and blade with the groove	144
4-11	Summary of Table 4-9 and Table 4-10	144

LIST OF FIGURES

1-1	Commercial helicopter and fixed-wing accident rate from 2008 to 2017	2
1-2	The accidents caused by the helicopter in the period of 1947 to 1996	3
1-3	The analysis of the cause helicopter accident by IHST	3
1-4	Dominant causal factors of the accident by AAIB	4
1-5	Phase of flight distribution accidents in the year 2000 to 2010 by EHEST	4
1-6	Retreating blade stall	6
2-1	Effect of blade number and chord on hover performance	11
2-2	SA Dauphin-365N with sweptback parabolic tip	12
2-3	Different tip shapes tested in S2 Chalais-Meudon wind tunnel	14
2-4	Effect of different tip shapes on hover performance	14
2-5	Effect of different tip shapes on cruise efficiency	15
2-6	Shapes of five different modified planform	16
2-7	Vertical flows for the BERP planform at high angle of attack	17
2-8	BERP blade geometry	18
2-9	Cambered aerofoil section distributions	18
2-10	Computed and experimental surface streamline patterns at high incidence and sweep	20
2-11	CFD Results for the flow separation near the notch region of a BERP blade	20
2-12	Stall area in yellow colour along the BERP aerofoil when the angles of attack increase (Re = 0.64x10^6, M = 0.2)	21
2-13	Particle trace of outboard flow field for both rotor and wing at 20 degrees	21

2-14	Cross-sectional view of flow field at two span-wise stations for both rotor and wing at 20 degrees	22
2-15	Various tip shapes assessed during BERP IV	23
2-16	Comparison of BERP III and BERP IV Tips (solid line is BERP IV and dotted line is BERP III)	24
2-17	Directed synthetic jet separation control concept	27
2-18	Implementation of a cylinder rotating valve for periodic bleed air modulation	27
2-19	Pulsed vortex generator jets	28
2-20	Baseline VR-12 aerofoil (a) Baseline Aerofoil (b) Droop Leading Edge	29
2-21	Comparison of the baseline SSC-A09 and 10o compliant dropped Spar85Def10 Section	29
2-22	Structural realization of Nose-Drooping design	30
2-23	Trailing edge devices: (a) Static Extended Trailing Edge (SETE), (b) Trailing Edge Flap (TEF), and (c) Gurney Flap (GF)	31
2-24	Trapped vortex concept	32
2-25	Kasper wing concept	32
2-26	Saab vortex Aerofoil	33
2-27	Lift coefficient Saab vortex aerofoil	33
2-28	EKIP aircraft	34
2-29	Wing with trapped vortex by moving circular cylinder	34
2-30	Lift coefficient versus angle of attack for airspeed V=60.96m/s	35
2-31	Schematic of flow development over aerofoil with step	35
2-32	Geometry of the modified NACA0024 with the vortex cell and the sketch of the wind tunnel test section	36
2-33	Sketch of the geometry of trapped vortex cell, reference system and location of the microphones for wall-pressure fluctuations measurements	37
2-34	Hybrid mesh of the aerofoil with cavity (left) and aerofoil with cavity for experimental setup (right)	38

2-35	Detail of suction slots inside the cavity of NACA0024	38
2-36	Vortex trapping with suction (a) Without suction (b) With suction, Q =0.02	39
2-37	Geometry of aerofoil with cavity using by Shengxian Shi *et al.*	40
2-38	Geometry of the NACA0018 aerofoil with cavity. The chord length is 165mm and the cavity opening of W =34 mm	40
2-39	Geometry of the flat plate wing model with no cavity (top) and triple cavities (bottom)	41
2-40	The computational domain and the geometry of the aerofoil with and without cavity	41
2-41	The geometry and meshing of the different cavity position at leading edge, mid chord and trailing edge	42
2-42	The geometry of the Riso_B1_18 aerofoil with cavity	43
3-1	Research methodology flowchart	49
3-2	Methodology diagram for development of Blade Element Theory code	50
3-3	Methodology diagram for Computational Fluid Dynamic analysis	51
3-4	Flow diagram of application of the Blade Element Theory on the helicopter blade.	53
3-5	Velocities distributed on the helicopter blade	55
3-6	Velocity components at blade element	57
3-7	Velocities at the blade in the plane of the disc	58
3-8	Velocities at the blade in the plane of flapping containing rotor axis and blade	58
3-9	Components of perpendicular velocity	59
3-10	Schematic diagram of the swashplate control system	62
3-11	Blade flapping motion	64
3-12	Rotor angle relationships	66
3-13	Angle of attack at blade element	67
3-14	Meshing of the blade movement area (rotor blade is divided into 50 elements along the span of the blade with equally	

	spaced azimuth angle spacing) (ψ = 7.2° each).	71
3-15	Flowchart for Blade Element Theory code	73
3-16	Flowchart of the simulation process	85
3-17	The steps in Pre-processing process	86
3-18	Aerofoil geometry (a) baseline NACA 0012 (b) modified NACA 0012 with vortex traps (aerofoil chord length, *c*, the location of the groove, *x*) (c) radius, *r*, of the groove	87
3-19	Computational domain for Baseline NACA0012 aerofoil and modified NACA 0012 aerofoil with a groove	88
3-20	Grid generation.	89
3-21	Transition to turbulence flow	90
3-22	Boundary layer grid comparison (a) unresolved boundary layer (b) resolved boundary layer	91
3-23	A complete view of the computation domain for a C-type mesh	92
3-24	The hybrid mesh around the NACA 0012 aerofoil with a single groove	93
3-25	Zoom of refined mesh around (a) leading edge, (b) trailing edge of the NACA0012 aerofoil and (c) refined mesh around the groove	94
4-1	Angle of attack and reverse flow area comparison. (a) Prouty's diagram (b) the computed analysis.	101
4-2	Rotation of main rotor blade.	102
4-3	Angle of attack and lift distribution for Blade A and B. (a) Angle of attack distribution (b) Lift distribution.	104
4-4	The effect of increasing forward speed of helicopter: Comparison of distribution angle of attack of the blade for forward speed at V =59.16m/s, V =80m/s and V =100m/s	106
4-5	The angle of attack distribution for forward speed V=59.16m/s, 80m/s and 100m/s at azimuth, ψ = 93.6° and 273.6°	107
4-6	Effect of increasing the collective pitch from 15.8° to 25° at forward speed V =59.16 m/s	108

4-7	Effect of increasing the collective pitch from 15.8° to 25° at forward speed V =80 m/s	109
4-8	Effect of increasing the collective pitch from 15.8° to 25° at forward speed V = 100m/s	110
4-9	The angle of attack distribution for forward speed V=59.16m/s in increment of the collective pitch angle at azimuth, ψ = 93.6° and 273.6°	111
4-10	Effect of increasing the twist angle of the blade from 0° to -10° at forward speed V =59.16 m/s	112
4-11	Effect of increasing the twist angle of the blade from 0° to -10° at forward speed V =80 m/s	113
4-12	Effect of increasing the twist angle of the blade from 0° to -10° at forward speed V =100 m/s	114
4-13	The angle of attack distribution for forward speed V=59.16m/s in changing of the twist angle of the blade at azimuth, ψ = 93.6° and 273.6°	115
4-14	(a) Top view of angle of attack contour of Prouty's helicopter in forward flight (b) Detail of distribution of angle of attack along the blade at advancing and retreating blade	117
4-15	Comparison of lift coefficient between experimental data and simulation results of six different turbulence models for NACA 0012 aerofoil M =0.3	120
4-16	Comparison between experimental data and six different simulation results of turbulence models of drag coefficient curve for NACA 0012 aerofoil M =0.3	120
4-17	Comparison of lift coefficient between experimental and numerical data for NACA 0012 Aerofoil M =0.35, Re = 3x10^6	122
4-18	Pressure coefficient of NACA 0012 M =0.35, α = 13.9, Re = 3 X 10^6	123
4-19	Fine meshing, $y^+ \approx 1$, δ =10 layers, and SR =1.2	125
4-20	Percentage of ΔC_l for different inflation layers and size of elements at α = 10deg, M =0.4	126
4-21	The flow of analysis of the groove	128

4-22	Comparison between numerical and experiment lift coefficient data at the tip of the helicopter blade r/R =1.0, M =0.4	129
4-23	Case (a): Effect of location $L1$ to $L4$ of the groove at radius $R1$=0.03c	130
4-24	Case (b): Effect of location $L1$ to $L4$ of the groove radius at $R2$=0.04c	131
4-25	Case (c): Effect of location $L1$ to $L4$ of the groove radius at $R3$=0.05c	131
4-26	Case (d): Effect of radius $R1$ to $R3$ of the groove at location $L1$=0.2c	133
4-27	Case (e): Effect of radius $R1$ to $R3$ of the groove at location $L2$=0.3c	133
4-28	Case (f): Effect of radius $R1$ to $R3$ of the groove at location $L3$=0.4c	134
4-29	Case (g): Effect of radius $R1$ to $R3$ of the groove at location $L4$=0.5c	134
4-30	Best radius of the groove for each location on the main rotor blade	135
4-31	Lift coefficient of the best configuration of location-radius of the groove on the aerofoil of main rotor blade	136
4-32	Change in lift coefficient, ΔC_l for the best configuration of location-radius of the groove on the aerofoil of main rotor blade	136
4-33	Lift coefficient of the groove $L4R3$ (0.5c & 0.05c)	137
4-34	Velocity contour for baseline aerofoil and aerofoil with the groove at various angles of attack	139
4-35	(a) Velocity contour, (b) Velocity Magnitude and (c) Streamline of the groove at 12 degrees angle of attacks	141
4-36	Pressure coefficient comparison between baseline aerofoil and aerofoil with single groove at $L4R3$, α =12 degrees	141
4-37	Pressure coefficient comparison between baseline aerofoil and aerofoil with single groove at $L4R3$, α =14 degrees	142

4-38	Comparison of the maximum of the angle of attack of the baseline aerofoil and aerofoil with the groove	145
4-39	Comparison of the maximum of the twist angle of the helicopter blade for the baseline aerofoil and aerofoil with the groove	146
4-40	Comparison of the maximum of the collective pitch angle of the baseline aerofoil and aerofoil with the groove	147

LIST OF SYMBOLS AND ABBREVIATIONS

SAR	Search and Rescue
GA	General Aviation
ASI	AOPA Air Safety Institute
IHST	International Helicopter Safety Team
FAA	Federal Aviation Administration
AAIB	Air accident investigation Branch
EHEST	European Helicopter Safety Team
BET	Blade Element Theory
BETC	Blade Element Theory Code
CFD	Computational Fluid Dynamic
V_{NE}	Never Exceed Speed
R	Blade radius
r	Radial distance to blade element
$\frac{r}{R}$	Radial station
θ	Blade section pitch
σ	Solidity $bc/\pi R^2$
θ_0	Blade pitch angle at hub
θ_1	Difference between hub and tip pitch angle
ρ	Mass density of air
V	True speed of helicopter along flight path
Ω	Rotor angular velocity
v	Induced inflow velocity at rotor
μ	Tip speed ratio $(V\cos\alpha/\Omega R)$
λ	Inflow ratio $(V\sin\alpha - v/\Omega R)$
ψ	Blade azimuth angle

U_T	Component at blade element of resultant velocity perpendicular to blade-span axis
U_P	Component at blade element of resultant velocity perpendicular both to blade-span axis and U_T
U_R	Component at blade element of resultant velocity parallel to blade-span axis and perpendicular to U_T
ϕ	Inflow angle at the blade element in plane perpendicular to blade-span axis $\left(\tan^{-1} U_P / U_T\right)$
α_r	Blade element angle of attack $(\theta + \phi)$
c_l	Section lift coefficient
a	Slope of curve of section lift coefficient against section angle of attack
β	Blade flapping angle at particular azimuth position
a_0	Constant term in Fourier series that express β (radians); hence, the coning angle
a_n	Coefficient of $\cos n\psi$ in expression for β
b_n	Coefficient of $\sin n\psi$ in expression for β
θ	Blade pitch angle at particular azimuth position
A_0	Constant term in Fourier series that express θ (radian); hence, the mean pitch angle representative radius
A_n	Coefficient of $\cos n\psi$ in expression for θ
B_n	Coefficient of $\sin n\psi$ in expression for θ
c	Chord of the aerofoil
f	Equivalent flat plate area
A	Area of disc
A_b	Area of blades
T	Thrust
g	Gravity
a	Lift curve slope
α_{TTP}	Tip path angle of attack

a_0	Coning angle
y^+	Distance of the first cell away from the wall
u_T	Friction velocity
μ	Fluid viscosity
S_m	Mass added to the continuous phase from the dispersed second phase
p	Static pressure
$\overline{\overline{\tau}}$	Stress tensor
$\rho\vec{g}$	Gravitational body force
$\vec{F}$	External body force
k_{eff}	Effective conductivity
k_t	Turbulent thermal conductivity
$\vec{J}_j$	Diffusion flux of species j
h	Enthalpy
Y_j	Mass fraction of species j
k	Turbulent kinetic energy
ω	Specific dissipation rate
Γ_k	Effective diffusivity of k
Γ_ω	Effective diffusivity of ω
Y_k	Dissipation of k due to turbulence
Y_ω	Dissipation of ω due to turbulence
$\tilde{G}_k$	The generation of turbulence kinetic energy due to mean velocity gradients.
G_ω	The generation of ω.
D_ω	The cross-diffusion term

σ_k	Turbulent Prandtl numbers for k
σ_ω	Turbulent Prandtl numbers for ω
S	Strain rate magnitude

LIST OF APPENDICES

APPENDIX	TITLE	PAGE
A	Algorithm for Blade Element Theory Code	169

CHAPTER 1

INTRODUCTION

1.1 Background study

The helicopter is a unique transport that is designed to perform at various flight maneuvers such as hovering as well as forward, rearward, sideward and vertical translations. Helicopters do not require a runway for take-off and landing and are also able to land almost everywhere. Thus, helicopters are a versatile mode of vehicle and are extensively used for missions such as air patrol, search and rescue (SAR), medical rescue missions, high-risk military missions, transportation to rural places or offshore missions and other missions of high risks.

However, the helicopter is dangerous compared to the fixed-wing. This was proven in the Report of General Aviation (GA) Accidents by AOPA Air Safety Institute (ASI) [1] as depicted in Figure 1-1. The accident rates of the helicopter increased rapidly compared to that of the fixed-wing, which declined severely from 2008 until 2016. From the years 2012 to 2016, the accident rate of the helicopter is higher than that of the fixed-wing. To be precise, in 2016, the highest rate of accidents for every 100,000 flight hours belongs to the helicopter, which is 2.69, whereas that of the fixed-wing was around 1.92. In other words, the risk of a helicopter crash versus that of the fixed-wing is about 29% greater per 100,000 hours in the air.

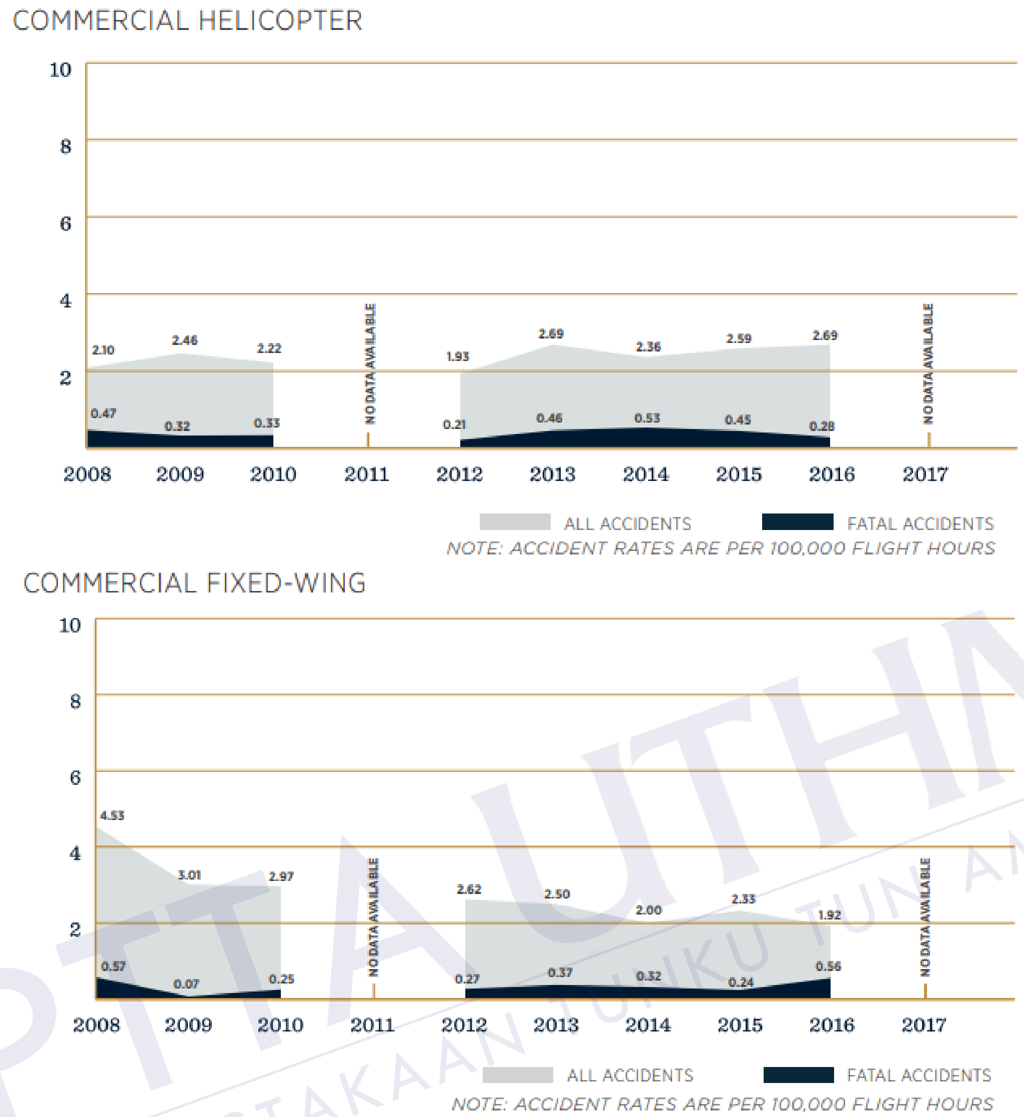

Figure 1-1: Commercial helicopter and fixed-wing accident rate from 2008 to 2017 [1].

There are four major factors shown in Figure 1-2 that contribute to the helicopter accidents, including the lack of engine airworthiness, non-engine airworthiness failures, maintenance-related failures and lastly, pilot errors/unknown causes [2]. These factors are based on 47 series of helicopter accidents for the period of 1947 through 1996. From these factors, the majority of accidents were due to pilot error/unknown causes. The pilot error refers to the U.S. rotorcraft accident data and statistics by the International Helicopter Safety Team (IHST), under Federal Aviation Administration (FAA) [3]. Reports show that the pilot error is divided into two main categories, namely pilot judgement/action problems and pilot situational awareness problems. The pilot awareness problems contribute to 34% of helicopter accidents

REFERENCES

[1] Aircraft Owners and Pilot Association Air Safety. *GA Accident Scorecard 2016-2017*. 2017.

[2] Fox, R. G. The history of helicopter safety. *International Helicopter Safety Symposium Montréal, Québec, Canada*. 2005.

[3] Federal Aviation Administration. *U.S. Rotorcraft Accident Data and Statistics*. 2012.

[4] Air Accidents Investigation Branch. *Annual Safety Review 2017*. 2018.

[5] European Helicopter Safety Team. *EHEST Analysis of 2006-2010 European helicopter accidents*. 2015.

[6] Federal Aviation Administration. Helicopter Emergencies and Hazards. , in *Helicopter flying handbook*, 2012, 1111–1124.

[7] National Transportation Safety Board. *Review of U.S Civil Aviation Accidents 2007-2009*. 2011.

[8] Department of the U.S. Army. Fundamentals of Flight. , in *Field Manual FM 3-04.203*, (May): , 2007

[9] Prouty, R. W. *Helicopter Performance, Stability and Control*. PWS Engineering Boston; 2002

[10] Nik Mohd, N. A. R. & Wahab, A. A. Feasibility study on improving of helicopter forward flight speed via modification of the blade dimension and engine performance,. *Proceeding of Rivet06, Kuala Lumpur*. 2006.

[11] Nik Mohd, N. A. R. Feasibility Study on Improving Of 5-Seater Helicopter Forward Flight Speed. Master's Thesis, Universiti Teknologi Malaysia. 2006.

[12] Mcveigh, Michael A, F. J. . Influence of tip shape , chord , blade number and airfoil on advanced rotor performance. *Journal of the American Helicopter Society*. 1984. 29(4): 55–62.

[13] Loftus, R. Swept tip design trade study - New affordable main rotor blade for the AH-64D Apache attack helicopte. *60th American Helicopter Society International Annual Forum , Baltimore, Maryland, USA*. 2004.

[14] Curtiss, H. . *et al.* Performance of a Sikorsky S-61 with a new main rotor. *Journal of American Helicopter Society*. 2003. 48(3): 211–215.

[15] Kondo, N. *et al.* Preliminary study of a low noise rotor. *54th Annual Forum of the American Helicopter Society*. 1998.

[16] Han, Y. O. & Leishman, J. . Investigation of helicopter rotor-blade-tip-vortex alleviation using a slotted tip. *Journal of AIAA*. 2004. 42(3): 524–535.

[17] Aoyama, T. *et al.* Effect of blade tip planform on shock wave of advancing helicopter blade. *Journal of Aircraft*. 1995. 32(5): 955–961.

[18] Yen, J. . Effects of blade tip shape on dynamics, cost, weight, aerodynamic performance, and aeroelastic response. *Journal of American Helicopter Society*. 1994. 39(4): 37–45.

[19] Mantay, W. R. & Yeager, W. T. J. Parametric tip effects for conformable rotor applications. *9th European Rotorcraft Forum, Stresa, Italy*. 1983. 53.1-53.29.

[20] Stalewski, W. & Zalewski, W. Performance improvement of helicopter rotors through blade redesigning. *Journal of Aircarft Engineering and Aerospace Technology*. 2019. 91(5): 747–755.

[21] Philippe, J.-J. ONERA makes progress in rotor aerodynamics, aeroelasticity, and acoustics. *Journal of American Helicopter Society*. 2000. 38(5): 48.

[22] Muller, R. H. G. *et al.* Blade deflection measurement of the low noise ERATO rotor. *26th European Rotorcraft Forum, The Hague, NL*. 2000. 104.1-104.9.

[23] Landgrebe, A. J. & Bellinger, E. Experimental investigation of model variable-geometry and ogee tip Rotors. *Technical Report NASA CR-227*. 1974.

[24] Gray, R. B. *et al.* Surface pressure measurements at two tips of a model helicopter rotor in hover. *Technical Report NASA CR-3281*. 1980.

[25] Huber, H. Helicopter flight characteristics improvement through swept-tip rotor blades. *5th European Rotorcraft and Power Lift Aircraft Forum, Amsterdam*. 1979. 29.1-29.20.

[26] Maskew, B. Influence of rotor blade tip shape on tip vortex shedding - an unsteady, inviscid analysis. *36th Annual Forum of the American Helicopter Society, Washington, DC*. 1980.

[27] Guilllet, F. & Philippe, J. J. Flight tests of a sweptback parabolic tip on a Dauphin-365N. *10th European Rotorcraft Forum, The Hague, The Netherlands*. 1984.

[28] Lafon, P. *et al*. *Ten years of rotor flow studies at ONERA : state of the art and future studies*. 1986.

[29] Wei, F. J. & Gunsallus, C. A new approach to rotor blade performance design improvement. *48th AIAA/ASME/ASCE/AHS/ASC Structures, Structural Dynamics and Marerials Conference*. 2007.

[30] Scott, M. T. *et al*. Computational and experimental evaluation of helicopter rotor tips for high-speed flight. *Journal of Aircraft*. 1991. 28(6): 403–409.

[31] Harrison, R. *et al*. BERP IV The Design , Development and Testing of an Advanced Rotor Blade. *American Helicopter Society 64th Annual Forum, Montreal, Canada*. 2008.

[32] Perry, F. . Aerodynamics of the Helicopter Speed Record. *American Helicopter Society 43rd Annual Forum*. 1987.

[33] Alan Brocklehurst & Duque, E. P. N. Experimental and numerical study of the british experimental rotor programme blade. *Journal of AIAA-90-3008-CP*. 1990.

[34] Nam, C. & Lee, D. Navier-stokes calculations of rotating berp planform blade flowfields. *Journal of AIAA-93-3527-CP*. 1993.

[35] Edwards, B. *et al*. Revolutionary concepts for helicopter noise reduction : SILENT program. *NASA Technical Report NASA/CR-2002-211650*. 2002.

[36] Beedy, J. *et al*. Experimental and CFD investigation of helicopter BERP tip aerodynamics. *Conference on Computational and Experimental Methods, University of Glasgow*. 2003.

[37] Tsung, F. & Sankar, L. N. Numerical simulation of flow separation for rotors and fixed wings. *Journal of AIAA 92-0635*. 1992.

[38] Amer, K. B. High speed rotor aerodynamics. *Journal of American Helicopter Society*. 1987. 34(1): 63.

[39] Caradonna, F. X. The application of CFD to rotary wing aircraft. *Technical Report NASA 102803*. 1992.

[40] Caradonna, F. . & Tung, C. Experimental and analytical studies of a model helicopter rotor in hover. *NACA Technical Memorandum 81232*. 1981.

[41] Carodonna & Tung. Experimental and analytical studies of a model helicopter in hover. *NASA Technical Memorandum 81232*. 1981.

[42] Mccroskey, W. J. Some Rototcraft Applications of Computational Fluid Dynamics. *NASA Technical Memorandum 100066*. 1988.

[43] Sidès, J. *et al.* Numerical simulation of flows around helicopters at DLR and ONERA. *Journal of Aerospace and Technology*. 2001. 5(1): 35–53.

[44] Ilkko, J. *et al.* Simulation of a helicopter rotor flow. *Journal of Structural Mechanics*. 2011. 44(3): 186–205.

[45] Chang, I. C. Transonic flow analysis for rotors. *NASA Technical Paper 2375*. 1990.

[46] Stalewski, W. Flow control on helicopter rotor blades via active gurney flap. *Journal of transactions on aerospace research*. 2018. 1(250): 98–118.

[47] Doerffer, P. & Szulc, O. Numerical simulation of model helicopter rotor in hover. *TASK Quarterly: Scientific Bulletin of Academic Computer Centre in Gdansk*. 2008. 12(3): 227–236.

[48] Rodriguez, C. *CFD analysis on the main-rotor blade of a Scale Helicopter Model using Overset Meshing*. KTH Royal Institute of Technology; 2012.

[49] Bailly, J. *et al.* Recent advances in rotor aerodynamic optimization, including structural data update. *Journal of American Helicopter Society*. 2017. 62

[50] Nik Mohd, N. A. R & Barakos G,N. Computational aerodynamics of hovering helicopter rotors. *Jurnal Mekanikal* 2012. (34): 16–46.

[51] Hassanzaded, D. & Mostofizadeh, A. R. Helicopter rotor airloads prediction using CFD and flight test in hover flight. *Journal of Aerospace Science and Technology*. 2012. 9(1): 37–48.

[52] Biava, M. *et al.* CFD prediction of air flow past a full helicopter configuration. *Journal of Aerospace Science and Technology*. 2012. 11–16.

[53] Biava, M. & Vigevano, L. Simulation of a complete helicopter : A CFD approach to the study of interference effects. *Journal of Aerospace Science and Technology*. 2012. (1): 37–39.

[54] Hariharan, N. *et al.* Simulation of rotor in hover : current state and challenges. *AIAA Journal*. 2014. (January):

[55] Barakos, G. & Steijl, R. Sliding mesh algorithm for CFD analysis of helicopter rotor–fuselage aerodynamics. *International Journal for Numerical Methods in Fluid*. 2008. (58): 527–549.

[56] Nakao, M. *et al.* Development of computational fluid dynamics method for helicopter rotor blade. *Mitsubishi Heavy Industries, Ltd. Technical Review*. 1997. 34(1):

[57] Caradonna, F. X. & Isomf, M. P. Subsonic and Transonic Potential Flow over

Helicopter Rotor Blades. *AIAA Journal*. 1972. 10(12): 1606–1612.

[58] Balaji, K. *et al.* Design and Development of Main Helicopter Rotor. *International Journal for Research in Applied Science & Engineering Technology*. 2017. 5(4): 74–77.

[59] Vladimirova, N. A. *CFD analysis and calculation of aerodynamic characteristics of helicopter rotor*. 2013.

[60] Perera, G. *et al.* Helicopter main rotor aerodynamic simulation with CFD. *Proceedings of Engineering , Build Environment and Spatial Science*. 2016. 144–150.

[61] Pandey, K. M. *et al.* Numerical Analyis of helicopter rotor at 400 RPM. *International Journal of Soft Computing and Engineering*. 2012. 2(1): 253–258.

[62] Yuksel, Al. Navier-Stokes Computations of Helicopter Rotor Flow Field. Master's Thesis, Middle East Technical University. 2017.

[63] Lonoce, M. Helicopter blade twist optimization in forward flight. *Master's Thesis, Instituto Superior Tecnico*. 2016.

[64] Cheeseman, I. C. & Seed, A. R. The application of circulation control by blowing to helicopter rotors. *Journal of the Royal Aeronautical Society*. 1967. 71(679): 451–467.

[65] McCormick, D. C. Boundary layer separation control with directed synthetic jets. *Journal of AIAA 2000-0519*. 2000.

[66] Lorber, P. *et al.* Retreating blade stall control. *Journal of AIAA 2000-2475*. 2000.

[67] Mccormick, D. C. *et al.* Compact, high-power boundary layer separation control actuation development. *Proceedings of ASME Fluids Engineering Division Summer Meeting*. 2001.

[68] Magill, J. *et al.* Dynamic stall control using a model-based observer. *Journal of Aircraft*. 2003. 40(2): 335–362.

[69] Martin, P. . *et al.* Dynamic stall measurements and computations for a VR-12 airfoil with a variable droop leading edge. *American Helicopter Society 59th Annual Forum, Phoenix, Arizona*. 2003.

[70] Kerho, M. Adaptive Airfoil Dynamic Stall Control. *Journal of Aircraft*. 2007. 44(4): 1350–1360.

[71] Geissler, W. *et al.* New rotor airfoil design procedure for unsteady flow

control. *26th European Rotorcraft Forum, The Hague, The Netherlands*. 2000.

[72] Geissler, W. & Trenker, M. Numerical investigation of dynamic stall control by a nose-drooping device. *American Helicopter Society Aerodynamics, Acoustics, and Test and Evaluation Technical Specialist Meeting, San Francisco, CA*. 2002.

[73] Chandrasekhara, M. S. *et al.* Unsteady stall control using dynamically deforming airfoils. *Journal of AIAA*. 1998. 36(10): 1792–1800.

[74] Léon, O. *et al.* Rotorcraft operating envelope expansion using extendable chord sections. *65th Annual Forum American Helicopter Society, Grapevine, Texas.* 2009.

[75] Liu, T. *et al.* Lift enhancement by static extended trailing edge. *Journal of Aircraft*. 2007. 44(6): 1939–1947.

[76] Yeo, H. Assessment of active controls for rotor performance enhancement. *Journal of the American Helicopter Society*. 2008. 53(2): 152–163.

[77] Lesieutre, G. A. Miniature trailing-edgeeffectors for rotorcraft. *Journal of the American Helicopter Society*. 2005. 52(2): 146–158.

[78] Bae, E.-S. *et al*. Optimally scheduled deployment of gurney flaps for rotorcraft power reduction. *65th Annual Forum Proceedings of the American Helicopter Society, Grapevine, Texas*. 2009. 171–95.

[79] VortexCell2050. Fundamentals of actively controlled flows with trapped vortices. *VortexCell2050 - Funded by the European Commission FP6 Programme*. 2007. 142–143.

[80] Kasper, W. . Some ideas of vortex lift. *Society of Automotive Engineers, Inc., Warrendale, PA,*. 1974. Paper 750512.

[81] Kruppa, E. W. Wind tunnel investigation of the kasper vortex concept. *AIAA 13th Annual Meeting and Technical Display Incorporating the Forum on the Future of Air Transportation*. 1977.

[82] Bunyakin, A. V *et al.* High-Reynolds-number batchelor-model asymptotics of a flow past an aerofoil with a vortex trapped in a cavity. *Journal of Fluid Mechanics*. 1998. 358(1): 283–297.

[83] Rossow, V. J. Lift enhancement by an externally trapped vortex. *Journal of Aircraft*. 1978. 15(9): 618–625.

[84] Fertis, D. G. New airfoil design concept with improved aerodynamic characteristics. *Journal of Aerospace Engineering*. 1994. 7(3): 328–339.

[85] Finaish, B. F. & Witherspoon, S. Aerodynamic performance of an airfoil with step-induced vortex for lift augmentation. *Journal of Aerospace Engineering*. 1998. 11(1): 9–16.

[86] Gregorio, F. De & Fraioli, G. Flow control on a high thickness airfoil by a trapped vortex cavity. *14th International Symposium on Laser Application to Fluid Mechanics, At Lisbon, Portugal*. 2008.

[87] Lasagna, D. *et al.* Effects of a trapped vortex cell on a thick wing airfoil. *Experiments in Fluids*. 2011. 51(5): 1369–1384.

[88] Lasagna, D. & Iuso, G. Flow regimes in a trapped vortex cell. *Experiments in Fluids*. 2016. 57(3): 1–20.

[89] Donelli, R. S. *et al. Optimization on thick airfoil to trap vortices*. 2008.

[90] Donelli, R. *et al.* Flow separation control by trapped vortex. *48th AIAA Aerospace Sciences Meeting Including the New Horizons Forum and Aerospace*. 2010.

[91] Donelli, R. S. *et al.* Suction optimization on thick airfoil to trap vortices. *XIX AIMETA (Italian Association of Theoretical and Applied Mechanics), Ancona, Italy*. 2009. 1–10.

[92] Tutty, O. R. *et al.* Control of flow with trapped vortices: Theory and Experiments. *International Journal of Flow Control*. 2013. 2(5): 89–109.

[93] Abdessalem, B. & Chernyshenko, S. On some stabilisation techniques of a trapped vortex. *3rd IASME/WSEAS International Conference on Fluid Dynamics & Aerodynamics, Corfu, Greece*. 2005. 84–89.

[94] Shi, S. *et al.* On the flow behaviour of a vortex-trapping cavity NACA0020 aerofoil at ultra-low Reynolds number. *17th International Symposium on Applications of Laser Techniques to Fluid Mechanics*. 2014. (2008): 1–12.

[95] J. Olsman, W. F. & Colonius, T. Numerical simulation of flow over an airfoil with a cavity. *Journal of AIAA*. 2012. 49(1): 143–149.

[96] Olsman, W. F. J. Influence of a cavity on the dynamical behaviour of an airfoil. PhD Thesis, Eindhoven University of Technology. 2010.

[97] Xi, T. S. *et al.* Flow visualisation study of wing-tip vortex for a wing with cavity. *Journal of Engineering and Applied Sciences*. 2017. 12(15): 3813–3817.

[98] Tee, Y. . Development of smoke wire system for vortex trapping application. Master’s Thesis, Universiti Sains Malaysia. 2015.

[99] Saeed, F. *et al*. Simulation of flow around a thick airfoil with a vortex trapping cavity. *11th International Conference of Numerical Analysis and Applied Mathematics*. 2013. 1558(1): 236–239.

[100] Bouferrouk, A. On the applicability of trapped vortices to ground vehicles. *International Vehicle Aerodynamics Conference*. 2015. 101–111.

[101] Puglisevich, L. S. Large eddy simulation for automotive vortical flows in ground effect. *PhD Thesis: Loughborough University*. 2013.

[102] Huncho, W.-H. *Aerodynamics of Road Vehicles*. Butterworth-Heinemann; 1987

[103] Wood, R. M. & Bauer, S. X. S. Simple and low-cost aerodynamic drag reduction devices for tractor-trailer trucks. *SAE International Truck and Bus Meeting and Exhibition, Fort Worth, Texas*. 2003.

[104] Garcia, D. L. & Katz, J. Trapped vortex in ground effect. *Journal of AIAA*. 2003. 41(4): 674–678.

[105] Katz, J. & Morey, F. Aerodynamics of large-scale vortex generator in ground effect. *Journal of Fluids Engineering*. 2008. 130(7): 1–6.

[106] Bouferrouk, A. *et al.* CFD simulations of crosswind impinging on a high speed train model. *18th Australasian Fluid Mechanics Conference*. 2012.

[107] Hemida, H. *et al.* The calculation of train slipstreams using large-eddy simulation. *Proceedings of the Institution of Mechanical Engineers, Part F: Journal of Rail and Rapid Transit*. 2014. 228(1): 25–36.

[108] Vuddagiri, A. & Samad, A. Vortex trapping by different cavities on an airfoil. *Wind Engineering*. 2013. 37(5): 469–482.

[109] Vuddagiri, A. *et al.* Flow analysis of airfoil having different cavities on its suction surface. *Progress in Computational Fluid Dynamics, An International Journal*. 2016. 16(2): 67.

[110] Fatehi, M. *et al.* Aerodynamic performance improvement of wind turbine blade by cavity shape optimization. *Renewable Energy an International Journal*. 2019. 132(1): 773–785.

[111] Leishman, J. G. *Principles of Helicopter Aerodynamics*. Cambridge University press; 2006

[112] Gessow, A. & Myers, G. C. *Aerodynamic of Helicopter*. Frederick Ungar Publishing Co. New York; 1999

[113] Johnson, W. *Helicopter Theory*. Dover Publications, Inc; 1980

[114] ANSYS Fluent (Version 12.0) User's Manual. *Fluent INC*

[115] Bardina, J. E. *et al*. Turbulence modeling validation, testing, and development. *NASA Technical Memorandum 110446*. 1997.

[116] Menter, F. . *et al*. Ten years of industrial experience with the SST turbulence model. *4th Internal Symposium, Turbulence, Heat and Mass Transfer , Antalya, Turkey*. 2003. 4(1): 625 – 632.

[117] Paul, J. c. Lift and profile-drag characteristic of an airfoil section as derived from measured helicopter rotor hovering performance. *NACA Technical Note 4357*. 1958.

[118] Department of Aerospace Engineering UIUC. UIUC Airfoil Coordinates Database. , 2018. .

[119] CFDOnline. CFD Online. , 2018. .

[120] Menter, F. R. Two-equation eddy-viscosity turbulence models for engineering applications. *Journal of AIAA*. 1994. 32(8): 1598–1605.

[121] Menter, F. Zonal two equation k-w turbulence models for aerodynamic flows. *NASA Technical Memorandum 111629*. 1993.

[122] Spalart, P. R. Trends in turbulence treatments. *Fluids 2000 Conference and Exhibit AIAA , Denver, Colo, USA*. 2000.

[123] Wells, J. *et al*. Effects of turbulence modeling on RANS simulations of tip vortices. *48th AIAA Aerospace Sciences Meeting Including the New Horizons Forum and Aerospace Exposition, Orlando, Florida*. 2010.

[124] Baldwin, B. S. & Barth, T. J. A one-equation turbulence transport model for high Reynolds number wall-bounded flows. *NASA Technical Memorandum 102847*. 1991.

[125] Spalart, P. & Allmaras, S. A one-equation turbulence model for aerodynamic flows. *30th AIAA Aerospace Sciences Meeting and Exhibit, Reno , USA*. 1994.

[126] Johansen, J. & Sorensen, J. N. Prediction of laminar turbulent transition in airfoil flows. *Journal of Aircraft*. 1999. 36(4): 731–734.

[127] Pettersson, K. & Rizzi, A. Comparing different CFD methods accuracy in computing local boundary layer properties. *Engineering Applications of Computational Fluid Mechanics*. 2009. 3(1): 98–108.

[128] Abbott, I. H. & Von Doenhoff, A. E. *Theory of Wing Sections: Including a Summary of Airfoil data*. Dover Publications, Inc; 1959